

Thermal Instability and Crystallization Characteristics of Amorphous Metal-Metalloid System

著者	MASUMOTO Tsuyoshi, WASEDA Yoshio, KIMURA Hisamichi, INOUE Akihisa
journal or publication title	Science reports of the Research Institutes, Tohoku University. Ser. A, Physics, chemistry and metallurgy
volume	26
page range	21-35
year	1976
URL	http://hdl.handle.net/10097/27748

Thermal Instability and Crystallization Characteristics of Amorphous Metal-Metalloid System*

Tsuyoshi MASUMOTO, Yoshio WASEDA**, Hisamichi KIMURA
and Akihisa INOUE

The Research Institute for Iron, Steel and Other Metals

(Received February 7, 1976)

Synopsis

Annealing effects on structure of several amorphous metal-metalloid systems (Pd-Si, Fe-P-C, Fe-Si-B, Co-Si-B and Ni-Si-B) were examined by electron microscopy, X-ray analysis and further by measurements of internal friction, electrical resistivity, specific gravity, microhardness and fracture strain. In T-T-T diagrams, distinct differences in transformation sequence were observed above and below the critical temperature. Above this temperature, crystallization proceeds through two metastable phases and finally to the stable phase by nucleation and growth mechanisms. Below this temperature, however, progressive aging gradually changes the structure through two stages; the initial stage is due to some degree of ordering in atomic arrangements in the as-quenched state and the subsequent stage due to transformation from amorphous to single phase with the same structure as the metallic element. A remarkable decrease in fracture strain of Fe-P-C alloys occurs after aging treatments at the incipient stage. This phenomenon is not a general character of all amorphous alloys.

I. Introduction

Most of noble or transition metals and its alloys containing about 20–25 at% of one or more kinds of metalloids such as P, C, B and Si are solidified in the amorphous phase by rapid quenching from the melts. Since the amorphous phase is thermodynamically unstable, transformation to stable crystalline phase should occur during heating above the temperature, so called “crystallization temperature”, which is inherent to respective alloys.⁽¹⁾ As to the crystallization although there have been a number of investigations⁽²⁾ for each individual amorphous alloy, general feature of the crystallization process has not been made clear, especially of the instability of amorphous phase at low temperatures. Recently, it has been noticed that distinct changes in some properties sensitive to the structure are induced by heating or aging even at temperatures appreciably lower than the crystallization temperature which is determined by means of X-ray

* The 1658th report of the Research Institute for Iron, Steel and Other Metals.

** The Research Institute of Mineral Dressing and Metallurgy

(1) Pol Duwez, *Trans. ASM*, **60** (1967), 607.

(2) For example: H. Jones and C. Suryanarayana, *J. Mater. Sci.*, **8** (1973), 705; H. Jones, *Rep. Progress Phys.*, **36** (1973), 1425; C.P. Peter Chou and D. Turnbull, *J. Non-cryst. Solids*, **17** (1975), 169.

and electron analyses.^{(3)~(9)}

The purpose of the present work is to present general information concerned with the thermal instability of amorphous phase and the transformation characteristics from amorphous to crystalline phase for several alloys of metal-metalloid system.

II. Experimental

The specimens used in the present work are Pd-Si, Fe-P-C, Fe-Si-B, Co-Si-B and Ni-Si-B alloys in the amorphous phase. These amorphous samples were prepared in shape of ribbons by rapid quenching from the melts using the centrifugal type and roller type quenching apparatuses.

The X-ray scattering experiment was carried out by using an automatic four-circle goniometer with a graphite monochromator and the Mo-K α radiation. The method of analyzing the X-ray scattering data was identical to that described previously.⁽¹⁰⁾ Microscopical examinations of the structural changes were performed by bright and dark field electron microscopy as well as ordinary electron diffraction using 100 kV electron microscope. Electrical resistivity measurements were carried out at liquid nitrogen temperature using a four-point-probe method, internal friction measurements using a K \bar{e} type microtorsion pendulum apparatus (0.5 Hz) and specific gravity using a usual method by electro-balance. Additional measurements were made with microhardness under a 100 g load and fracture strain by bending method which was the same as that described by Graham *et al.*⁽⁶⁾

III. Results and discussion

1. Amorphous structure and disorder parameter determined by X-ray analysis.

As is well-known the structure factor $S(Q)$ of the amorphous alloys shows only a few broad peaks, similar to that of the liquid alloys.⁽¹⁾ Fig. 1 shows the structure factor of amorphous $M_{78}\text{-Si}_{10}\text{-B}_{12}$ alloys ($M=\text{Fe, Co and Ni}$) obtained in this work. In order to compare the amorphous state with the liquid state, the structure factors of liquid Fe, Co and Ni near the melting points⁽¹¹⁾ are also

(3) H. Fujimori, T. Masumoto, Y. Obi and M. Kikuchi, Japan. J. Appl. Phys., **13** (1974), 1889.

(4) T. Egami, P.J. Flanders and C.D. Graham, Jr., AIP Conf. Proc., **24** (1975), 697.

(5) F.E. Luborsky, J.J. Becker and R.O. McCary, Trans. on Magnetism, (1975) in press (Technical Information Series of GE, No. 75CRD134 (1975).)

(6) C.D. Graham, Jr., T. Egami, R.S. Williams and Y. Takei, 3M Conf. Proc., (1975) in press.

(7) H.S. Chen and E. Coleman, Appl. Phys. Lett., (1976) in press.

(8) H.S. Chen, Scripta Met., **9** (1975), 411.

(9) H.S. Chen, S.D. Ferris, E.M. Gyorgy, H.J. Leamy and R.C. Scherwood, Appl. Phys. Lett., **26** (1975), 405.

(10) Y. Waseda and T. Masumoto, Z. Physik, **B22** (1975), 121.

(11) Y. Waseda and S. Tamaki, Phil. Mag., **32** (1975), 273.

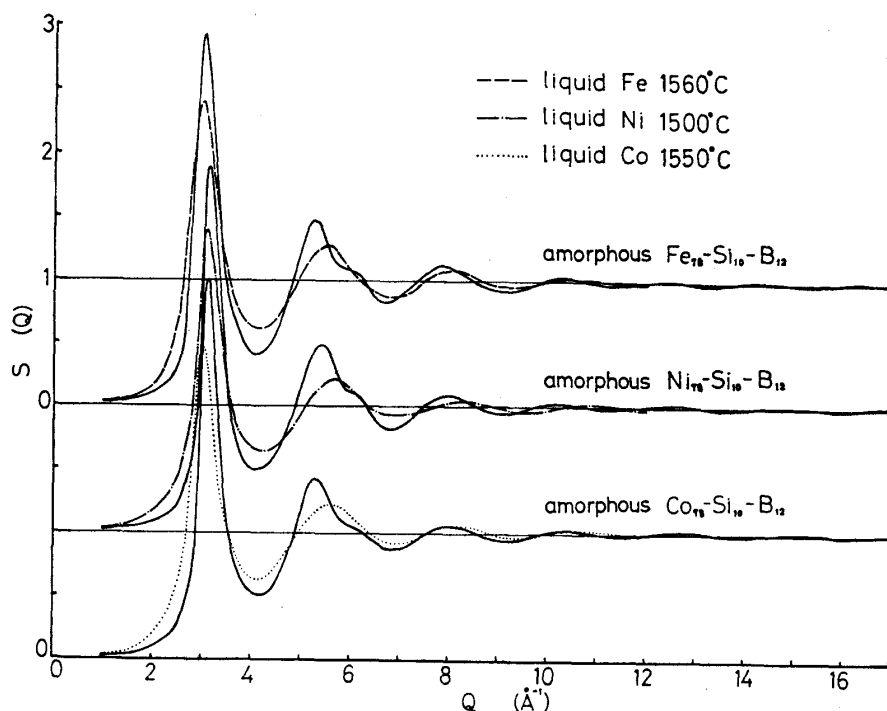


Fig. 1. Structure factor of amorphous $M_{78}\text{-Si}_{10}\text{-B}_{12}$ alloys ($M=\text{Fe}, \text{Co}$ and Ni) and liquid Fe, Co and Ni .

plotted in Fig. 1. The essential feature of the structure factor for the amorphous alloys is the same as those of the liquid pure metals (M) excepting for the split second peak. As seen in this figure the oscillation of the structure factor of the liquid state decays more rapidly in a high Q region. However, in the case of the amorphous state, the oscillation is evidently retained to a high Q region in comparison to the liquid state. The same results are also observed in the pair distribution function $g(r)$ which is the Fourier transform of the structure factor (see Fig. 2). From these facts it is suggested that there should be some difference in the disordered atomic distribution between amorphous and liquid states.

In the field of the structural study of amorphous alloys, a measure of the structural disorder seems to be one of the most important informations. However, no definite answer to this problem is available at present. In this work, a semi-empirical approach for estimating the region of short range order was performed by using the experimental data of the pair distribution function. We introduce by r_s the range of r , beyond which the short range order disappears and $g(r)=1\pm 0.02$. The fluctuation of ± 0.02 is considered to be reasonable from the errors in $g(r)$ at large r . This assumption requires that r_s must become small if the nature of disordering is dominant. In the extreme cases, r_s is infinite in crystalline state whereas r_s is equal to the nearest neighbour distance in gaseous state. With the value of r_s , a dimensionless parameter for the structural disorder is defined as

$$\zeta = r_s/r_1,$$

where r_1 is the nearest neighbour distance. Table 1 shows the parameter ζ of

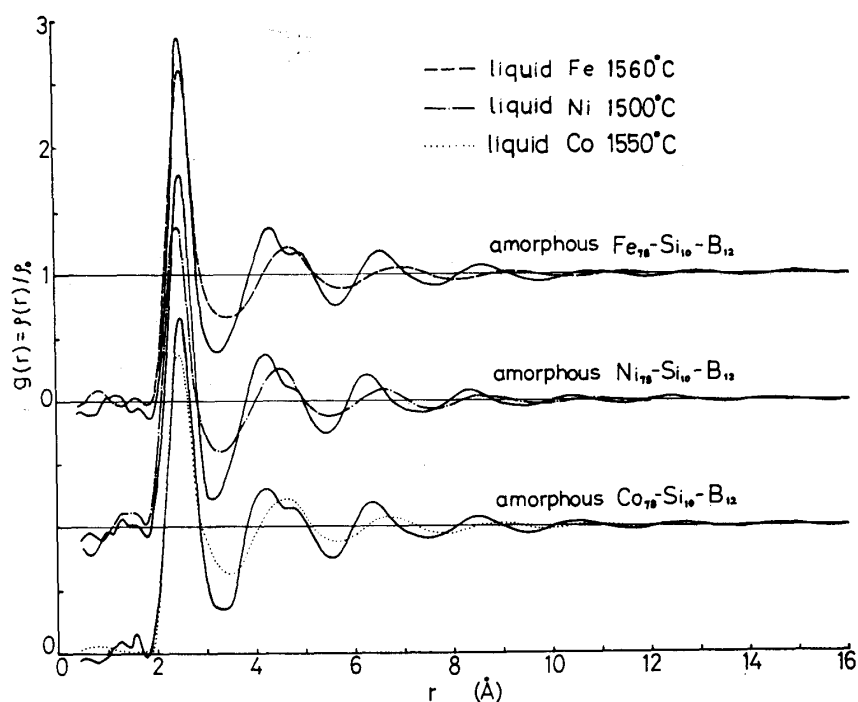


Fig. 2. Pair distribution function of amorphous $M_{78}\text{-Si}_{10}\text{-B}_{12}$ alloys ($M=\text{Fe}$, Co and Ni) and liquid Fe , Co and Ni .

Table 1. Changes in the disorder parameter ζ estimated from experimental structural data for various alloys in amorphous and liquid states.

	$r_1(\text{Å})$	$r_s(\text{Å})$	ζ
$\text{Pd}_{80}\text{-Si}_{20}$			
amorphous	2.81	16.0	5.69
liquid	2.76	11.5	4.17
$\text{Fe}_{80}\text{-P}_{18}\text{-C}_7$			
amorphous	2.58	15.0	5.81
liquid	2.58	11.0	4.26
amorphous			
$\text{Fe}_{78}\text{-Si}_{10}\text{-B}_{12}$	2.58	15.0	5.81
$\text{Co}_{78}\text{-Si}_{10}\text{-B}_{12}$	2.53	14.5	5.73
$\text{Ni}_{78}\text{-Si}_{10}\text{-B}_{12}$	2.55	14.5	5.69
liquid			
Fe	2.58	10.5	4.07
Co	2.56	11.0	4.30
Ni	2.53	10.5	4.15

several amorphous alloys estimated from the experimental data of $g(r)$. As shown in this table, the parameter of amorphous alloys is about 5.7 times the nearest neighbour distance, and this is larger than that (about 4.2) of liquid metals. The results in the table also indicate that the parameter of amorphous alloys is independent of the alloy concentrations. From this point, when the amorphous

samples have ζ of the same order the structural disorder may be quite similar, within the first approximation, in these amorphous alloys.

2. Crystallization process.

During the heating treatment the amorphous phase transfers progressively to a fully stable phase through a sequence of more stable phases, rather than directly. For instance⁽¹²⁾, the transformation sequence in amorphous $\text{Pd}_{80}\text{Si}_{20}$ alloy has been identified as consisting of the following four successive stages; (1) the incipient stage of crystallization (Am') during which some degree of ordering occurs in the atomic arrangements of the amorphous phase, (2) the appearance of a number of small Pd crystallites with a fcc structure within the amorphous matrix (MS-I), (3) the formation of a complex ordered metastable phase (MS-II) over the entire amorphous matrix with dispersed MS-I phase, and (4) the final stage to produce the stable phase (ST) consisting of Pd and Pd_3Si . It has been also found in this alloy that a prolonged annealing at the incipient stage of crystallization induces a change from amorphous phase to supersaturated metastable phase (SS) of a fcc microcrystalline assembly.⁽¹³⁾

Such a transformation sequence which has been found for the Pd-Si system was nearly similar to those for other amorphous alloys⁽¹⁴⁾ employed in the present study. The representative transformation sequence is illustrated in Fig. 3, and the characteristics of phases at each stage are summarized in Table 2 for every amorphous alloys studied.

In order to clarify in more detail the characteristics of transformation, the

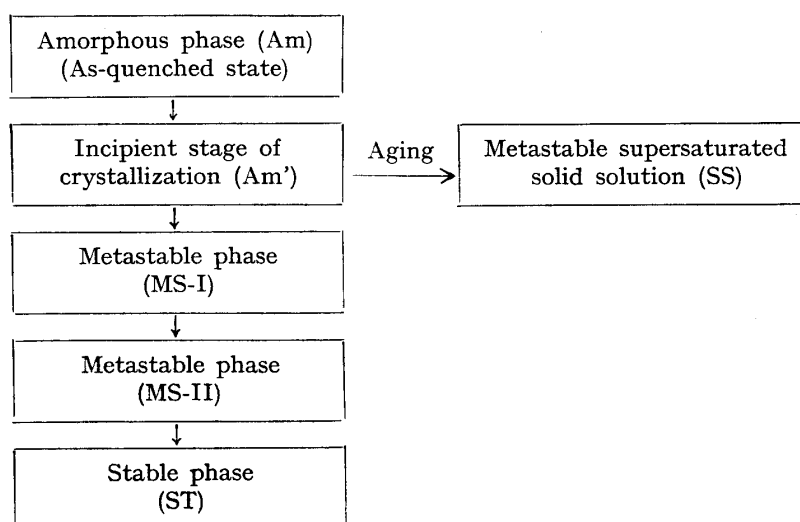


Fig. 3. Systematic transformation sequence of amorphous metal-metalloid alloys used in the present work.

(12) T. Masumoto and R. Maddin, *Acta Met.*, **19** (1971), 725.

(13) R. Maddin and T. Masumoto, *Mater. Sci. Eng.*, **9** (1972), 153.

(14) T. Masumoto and Hiroshi Kimura, *J. Japan Inst. Met.*, **39** (1975), 273; *Sci. Rep. RITU A-Vol.* **25** (1975), 216.

Table 2. Characteristics of phases at each stage for various amorphous alloys

Phase	Pd ₈₀ Si ₂₀	Fe ₈₀ P ₁₃ C ₇	Fe ₇₈ Si ₁₀ B ₁₂	Co ₇₅ Si ₁₅ B ₁₀	Ni ₇₅ Si ₈ B ₁₇
SS	fcc (a=3.921Å)	bcc (a=1.861Å)	bcc (a=2.848Å)	hcp (a=2.161Å) c=4.041Å)	fcc (a=3.508Å)
MS-I	fcc (a=3.89Å)	bcc (a=2.87Å)	bcc (a=2.87Å)	hcp (a=2.16Å) (c=4.04Å)	fcc (a=3.52Å)
MS-II	(Complex ordered phase ?)				
ST	Pd, Pd ₃ Si	Fe, Fe ₃ C Fe ₃ P	Fe, Fe ₃ Si Fe ₂ B	Co, Co ₃ B Co ₃ Si	Ni, Ni ₃ B Ni ₃ Si
T _c	380°C	410°C	505°C	480°C	482°C
T _c '	250°C	350°C	—	375°C	360°C

T_c: Crystallization temperature, at which the exothermic peak begins to appear at a scanning rate of 5°C/min.

T_c': Critical temperature, below which the SS phase appears.

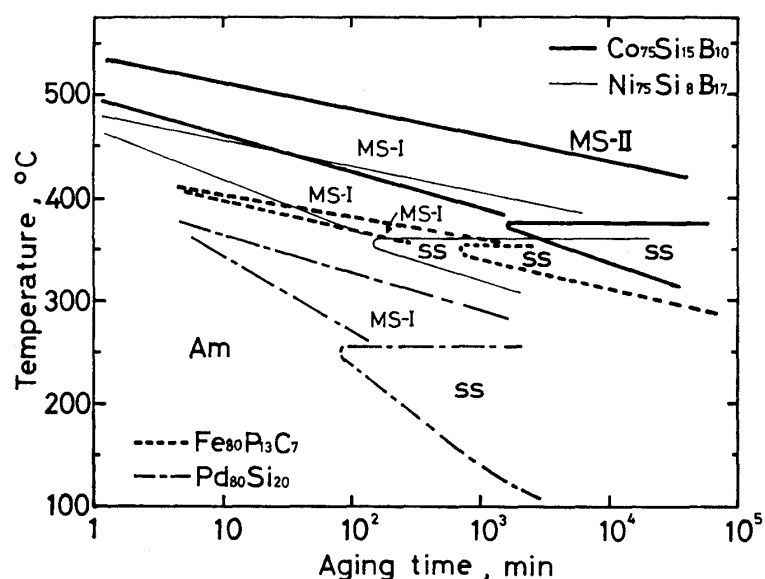


Fig. 4. Time-temperature-transformation diagrams of four amorphous alloys.

time-temperature-transformation diagram of each amorphous alloy was constructed by using transmission electron microscopy, X-ray and electron diffraction methods. As a result a coherent picture of the T-T-T diagram was obtained for all amorphous alloys used in the present work. Fig. 4 illustrates the T-T-T curves for four amorphous alloys, in which each phase corresponds to each crystallization sequence shown in Fig. 3. In this figure, distinct differences in the transformation process and mode are observable beyond and below the critical temperature, T_c' . Above this temperature the crystallization proceeds through the two metastable phases and finally to the stable phase by the nucleation and growth mechanisms. Below

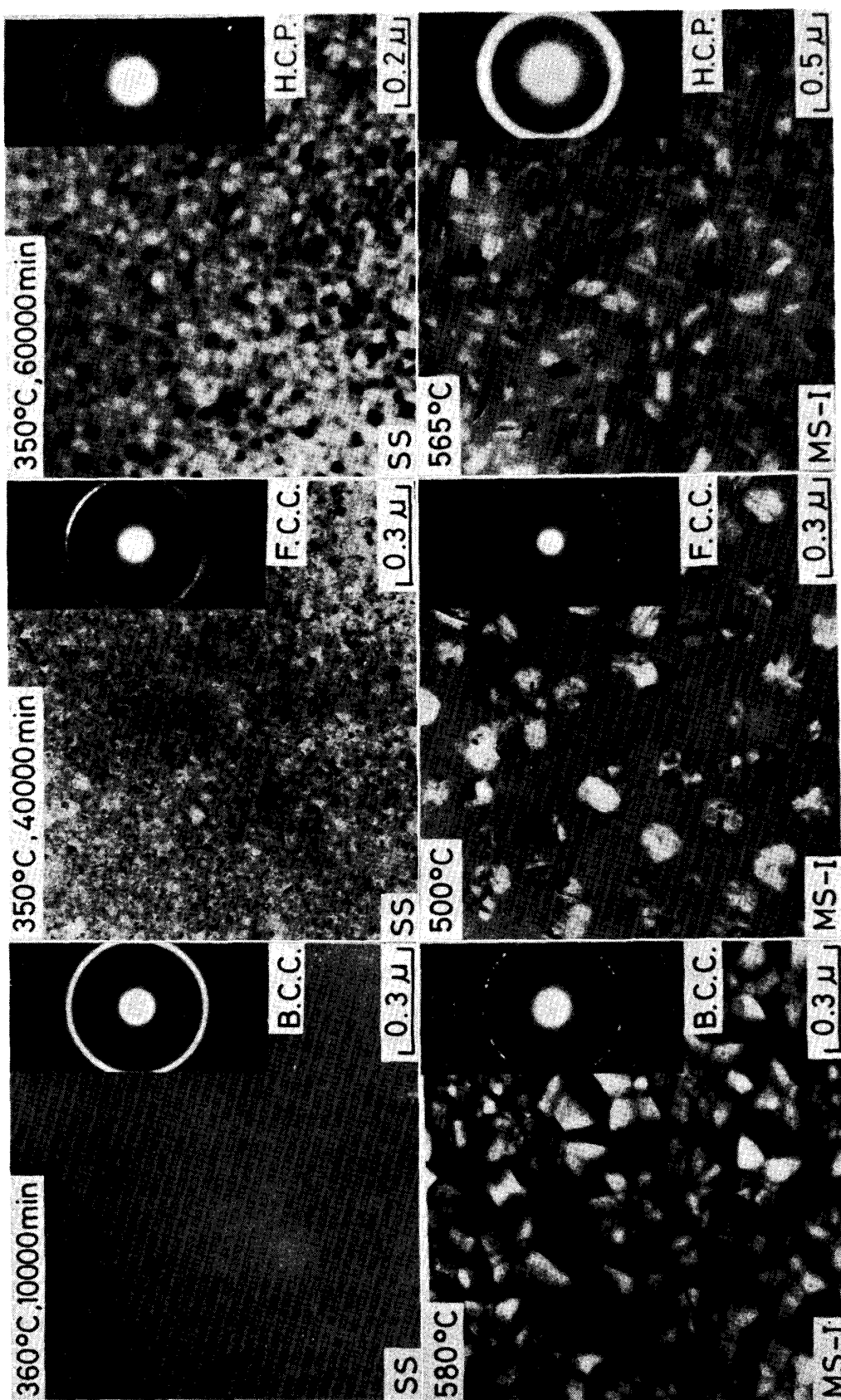
T_c' , however, progressive aging changes gradually the structure from amorphous to single phase (SS). As seen in Table 2, this phase has the same structure as that of the major metallic element, i.e. a fcc structure in Pd-base and Ni-base alloys, a bcc structure in Fe-base alloys and a hcp structure in Co-base alloys. These phases are highly stable after long aging below the critical temperature and consist of an assembly of microcrystallites. Photo. 1 shows the transmission electron micrographs and electron diffraction patterns of the MS-I and SS phases after aging beyond and below T_c' . Although the two phases have the same crystal structure, the transformation mode is different; i.e. the MS-I phase precipitates within amorphous matrix distinctly by the nucleation and growth mechanisms, while the SS phase grows gradually into an assembly of microcrystallites having diameters of about 50~100 Å over the entire matrix. Judging from the lattice constant of these phases it is suggested that the former is a phase consisting of nearly pure metallic element, and the latter is a supersaturated solid solution with the same composition as that of the matrix.

3. Thermal instability of amorphous structure at incipient stage of crystallization.

It is essential to examine carefully the incipient stage of crystallization in order to understand the thermal instability of amorphous alloys. From this point of view more detailed investigations of this stage were made by electron microscopy, X-ray analysis and further by measurements of specific gravity, internal friction, electrical resistivity, microhardness and fracture strain in bending.

Figs. 5 and 6 show the structure factor and pair distribution function of Pd-Si alloys aged for various times at 200°C. A slight change is observed even within 200 min; the first peak becomes sharper and the splitting of second peak becomes less distinct. Upon further aging several new peaks superimpose on the original pattern of the amorphous phase, and these new peaks become continuously sharper with increasing aging time. These data are quite similar to those of Fe-P-C alloy reported in the previous work.⁽¹⁰⁾ The positions of the new peaks coincide with those of atoms in fcc structure with a lattice constant $a=3.92$ Å, and are indicated by the vertical lines. Table 3 shows the aging time dependence of the disorder parameter ζ estimated from the distribution functions. The parameter increases slightly with aging time in the range of 30 to 200 min, then abruptly increases above 200 min at which several peaks of a fcc structure appear on the X-ray pattern. In Fig. 7 the changes in the disorder parameter ζ of Pd-Si alloy are represented in the T-T-T diagram as functions of temperature and aging time. The crystallization occurs on a line of about 7 in the parameter ζ .

According to transmission electron microscopy, no evidence of crystallization is detectable in the structure of Pd-Si alloys aged within 200 min. By aging longer than 200 min, however, a large number of granular crystallites can be observed in electron micrographs. In the dark field images shown in Photos. 2 and 3 as several examples, the shape and contrast of microcrystallites become continuously



$Fe_8Si_{10}B_{12}$ Alloy
 $Ni_{75}Si_8B_{17}$ Alloy
 $Co_{75}Si_{15}B_{10}$ Alloy
 Photo. 1. Electron micrographs of SS phase and MS-I phase for Fe-Si-B, Ni-Si-B and Co-Si-B alloys.

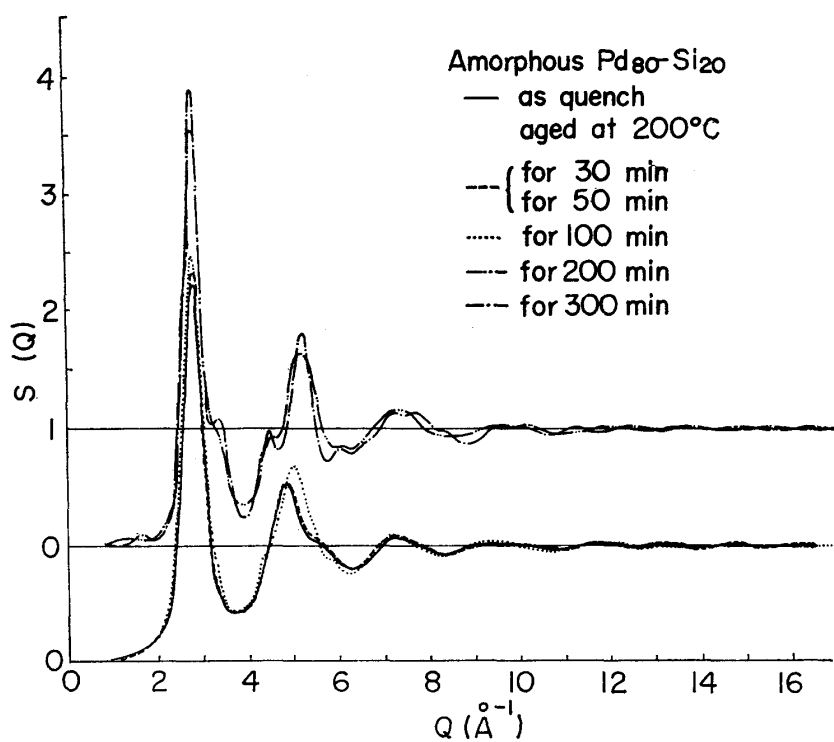


Fig. 5. Structure factor of $\text{Pd}_{80}\text{-Si}_{20}$ alloys aged at 200°C for various times.

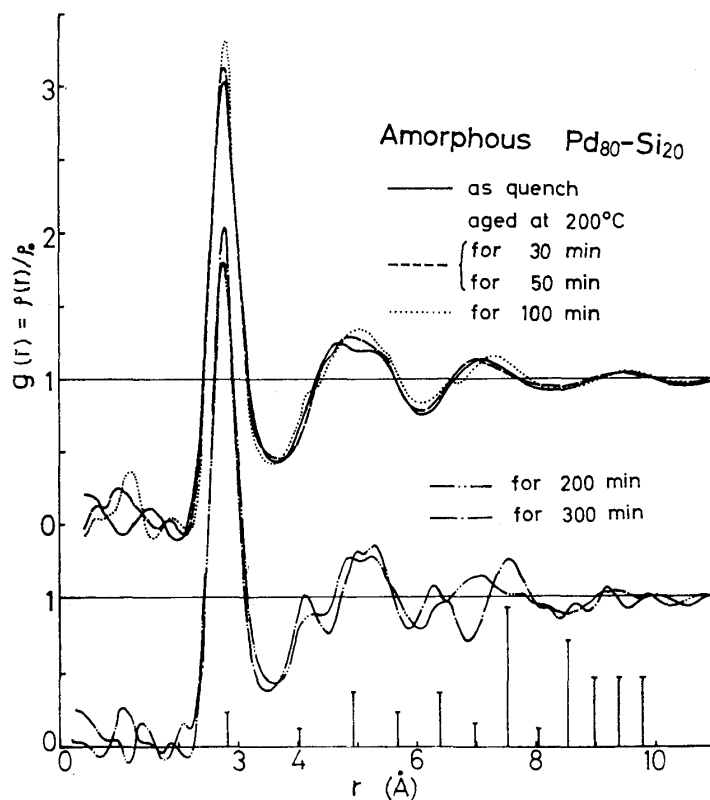


Fig. 6. Pair distribution function of $\text{Pd}_{80}\text{-Si}_{20}$ alloys aged at 200°C for various times.

Table 3. Changes in the disorder parameter ζ estimated from experimental structural data for amorphous $\text{Pd}_{80}\text{-Si}_{20}$ during isothermal aging at 200°C.

Aging time (min)	r_s (Å)	ζ
0	16.0	5.69
30	16.0	5.69
50	16.5	5.87
100	17.0	6.05
200	18.5	6.58
300	22.5	8.01

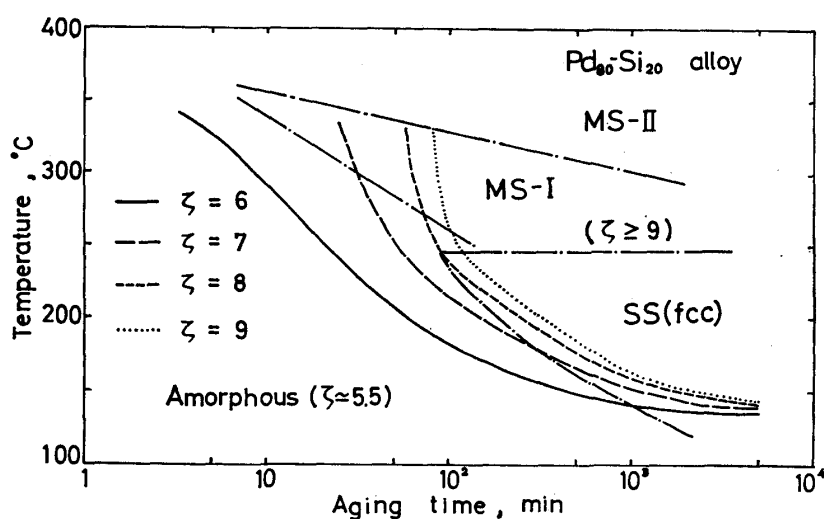


Fig. 7. Changes in the disorder parameter ζ of $\text{Pd}_{80}\text{-Si}_{20}$ alloy in T-T-T diagram.

more distinct with increasing aging time and subsequently the structure shows an assembly of well-defined crystallites having a diameter of about 100 Å over the entire matrix.

The similar results were obtained for other amorphous alloys. As a general feature it can be said that there are two stages in the structural change by aging at lower temperatures. The initial stage corresponds to the incipient stage of crystallization (Am'), during which some degree of ordering in the short range occurs in the amorphous phase. At the subsequent stage the amorphous structure transforms to the single phase (SS) which has the same structure as the constituent metal. Although the precipitation mechanism of the single phase is not clear, it is proposed from X-ray and electron microscopic analyses that the crystallization will take place in a manner of continuous growth, that is, the short range ordered clusters which are prepared at the incipient stage of crystallization are gradually rearranged into a well-defined crystal structure without a long range diffusion of atoms.

In the recent works,^{(3)~(7)} it has been found that some amorphous alloys

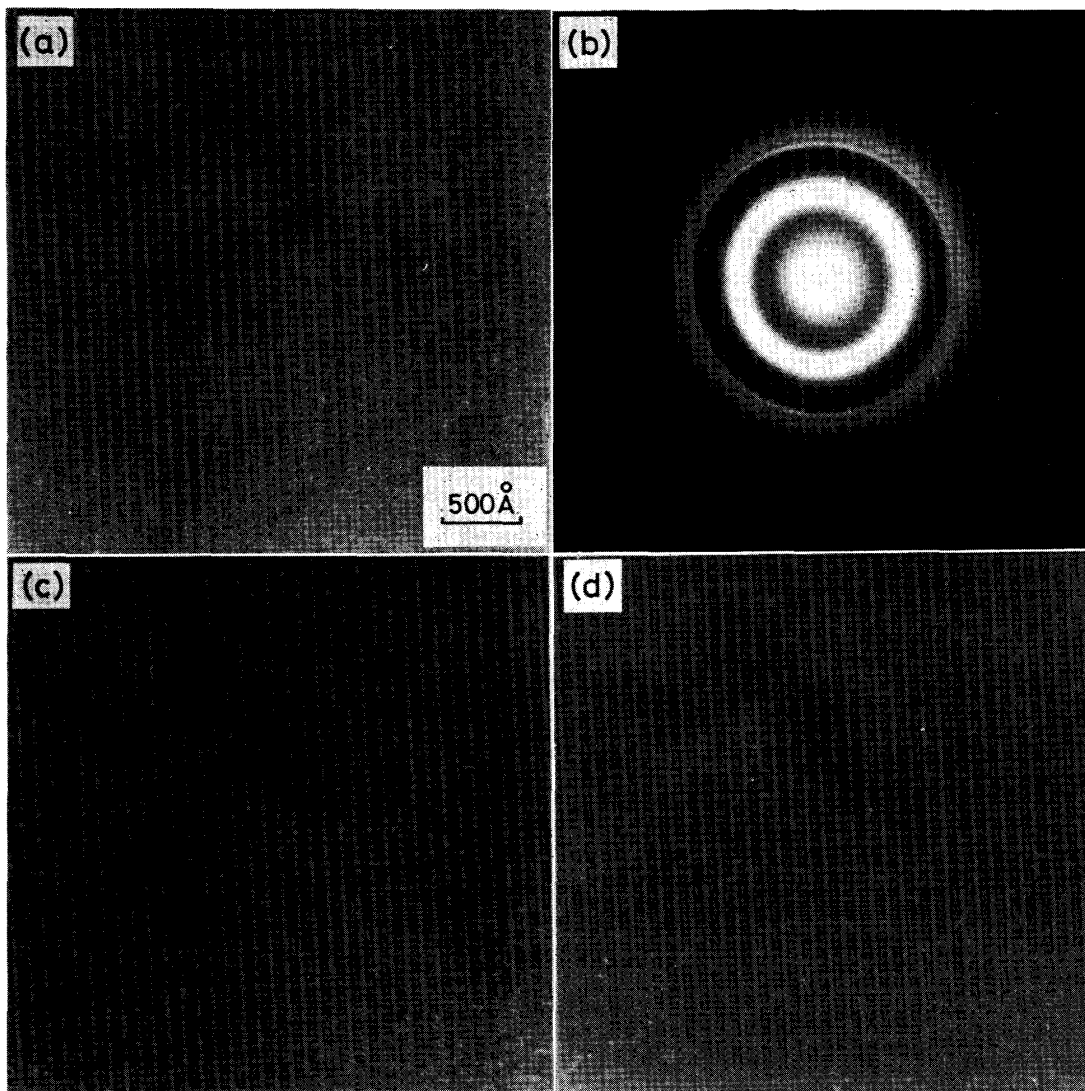


Photo. 2. Transmission electron micrographs showing the single phase with a fcc structure of amorphous $\text{Pd}_{80}\text{-Si}_{20}$ alloy aged for 2500 min at 200°C . (a) bright field image; (b) its associated diffraction pattern; (c) dark field image taken by displacing an objective aperture on the first halo of diffraction pattern containing 111 and 200 reflection rings of fcc phase; (d) dark field image taken by displacing an objective aperture on 220 reflection ring of fcc phase.

have larger magnetic anisotropies and that the magnitude of these anisotropies is decreased by annealing at temperatures too low to cause crystallization. The origin of this magnetic anisotropy has been thought to involve anisotropies in short range structural or compositional ordering⁽¹⁵⁾ and/or internal strains^{(3)~(7)} arising from the rapid quenching. If these anisotropies or internal strains are present in the as-quenched specimen, they may be relaxed during annealing at the incipient stage of crystallization. Recently, Graham et al.⁽⁶⁾ have found that

(15) G.C. Chi and G.S. Cargill III, Proc. of 2nd Intern. Conf. on Rapid Quenched Metals, Boston, Mass., (1975), in press.

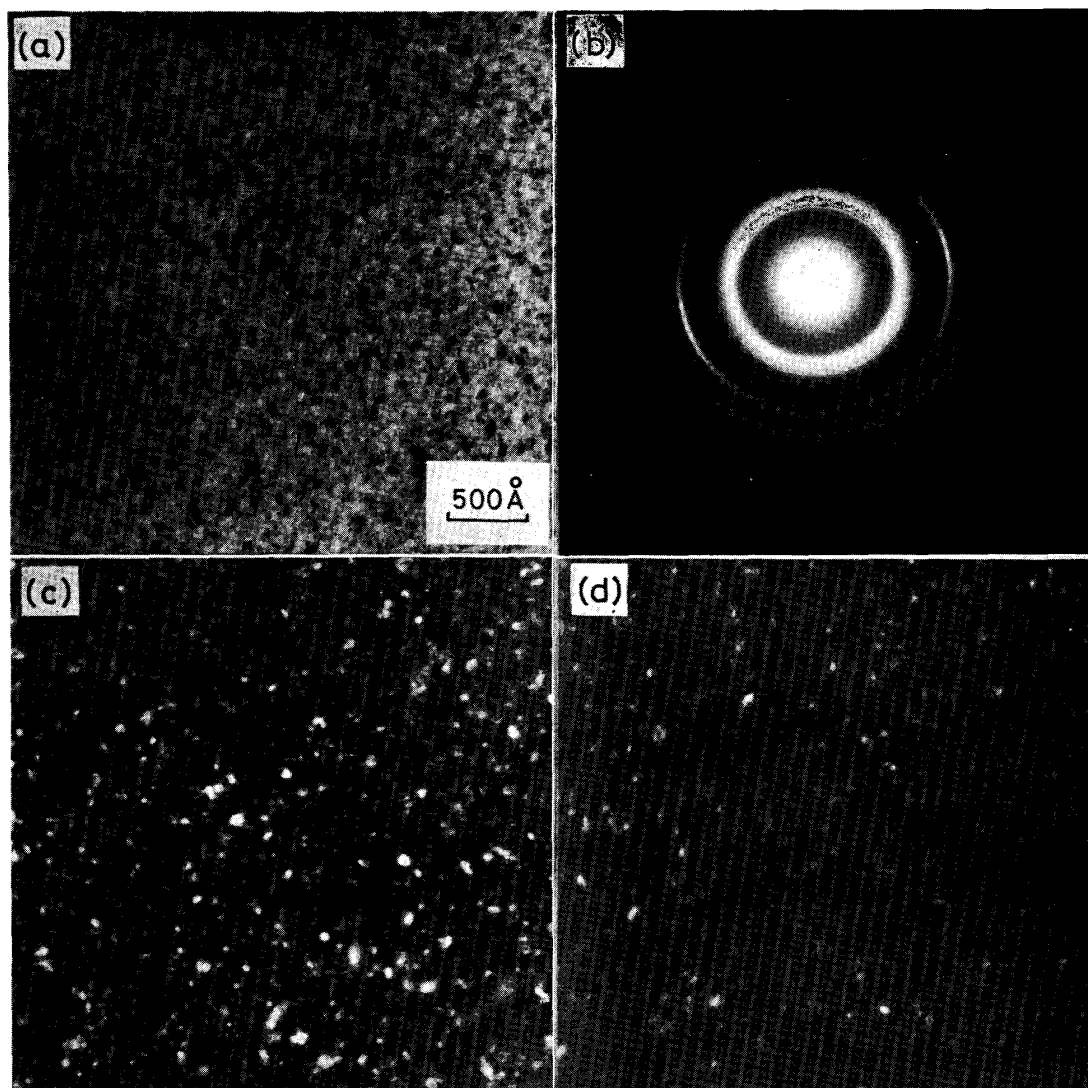


Photo. 3. Transmission electron micrographs showing the single phase with a fcc structure of amorphous $\text{Pd}_{80}\text{Si}_{20}$ alloy aged for 18000 min at 200°C . (a) bright field image; (b) its associated diffraction pattern; (c) dark field image taken by displacing an objective aperture on 111 and 200 reflection rings of fcc phase; (d) dark field image taken by displacing an objective aperture on 200 reflection ring of fcc phase.

changes in the stress relaxation and fracture strain obtained by bending test occur in qualitatively similar way to that in the magnetic anisotropy at lower temperatures. From these results they have assumed that the same atomic rearrangements are responsible for all three quantities.

In order to clarify such annealing effects, the changes in various physical and mechanical properties were examined with Pd-Si and Fe-P-C alloys aged at low temperatures. These results are summarized in Figs. 8 and 9 together with the results of the disorder parameter ζ . In Fig. 8, at the incipient stage of crystallization (below about 200 min), the internal friction and electrical resistance

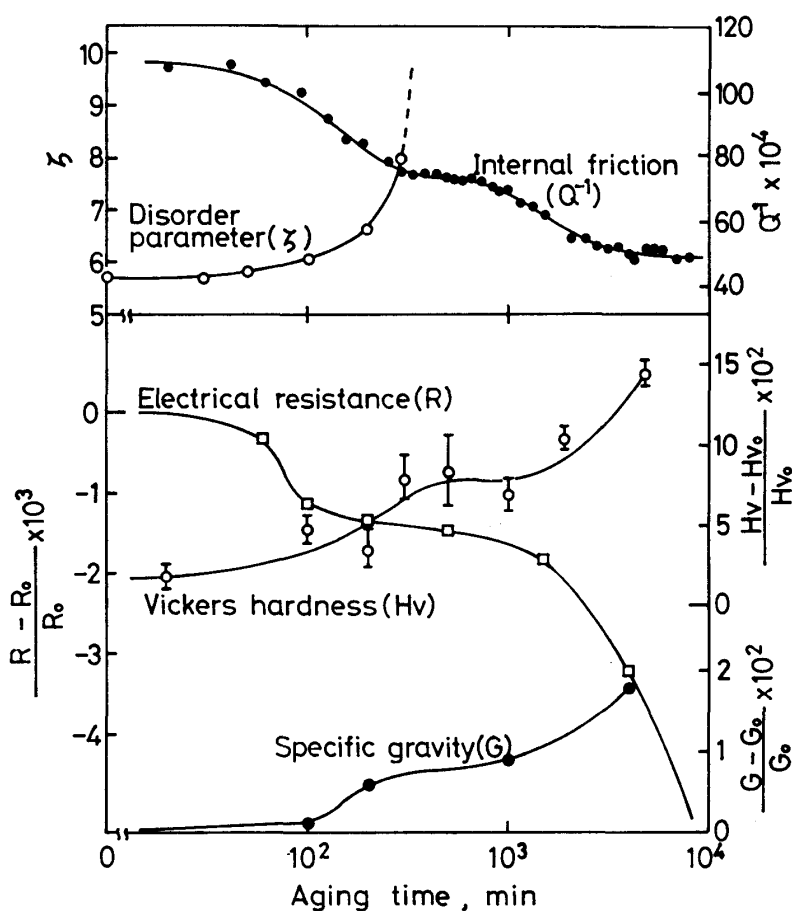


Fig. 8. Changes in various properties of $\text{Pd}_{80}\text{-Si}_{20}$ alloy during aging at 200°C .

decrease appreciably, while the specific gravity and microhardness increase only slightly. Transformation of amorphous phase to the microcrystalline phase by further aging treatments results in remarkable changes in all quantities. It is found that the former quantities are more sensitive to the atomic rearrangement in the short range order in comparison to the latter ones. The similar phenomena are also found in the internal friction and hardness for Fe-P-C alloys as shown in Fig. 9. In these two figures, it should be notice moreover that the behaviors of fracture strain during aging differ in these two alloys: in the Fe-P-C alloys a significant decrease of fracture strain occurs within very short times of the incipient stage, although in the Pd-Si alloys no change is detected even after long times during which crystallization occurs clearly.

Various experimental facts described above may lead to the following conclusions. The aging treatments at lower temperatures cause some ordering of atoms in the short range, resulting in the relaxation of internal strains or anisotropic configuration of atoms arising from the rapid quenching. Such atomic rearrangements are reflected in changes of the structure-sensitive properties such as electrical resistivity and internal friction. On the other hand, a remarkable decrease in the fracture strain of Fe-P-C alloys seems to be due to a certain change

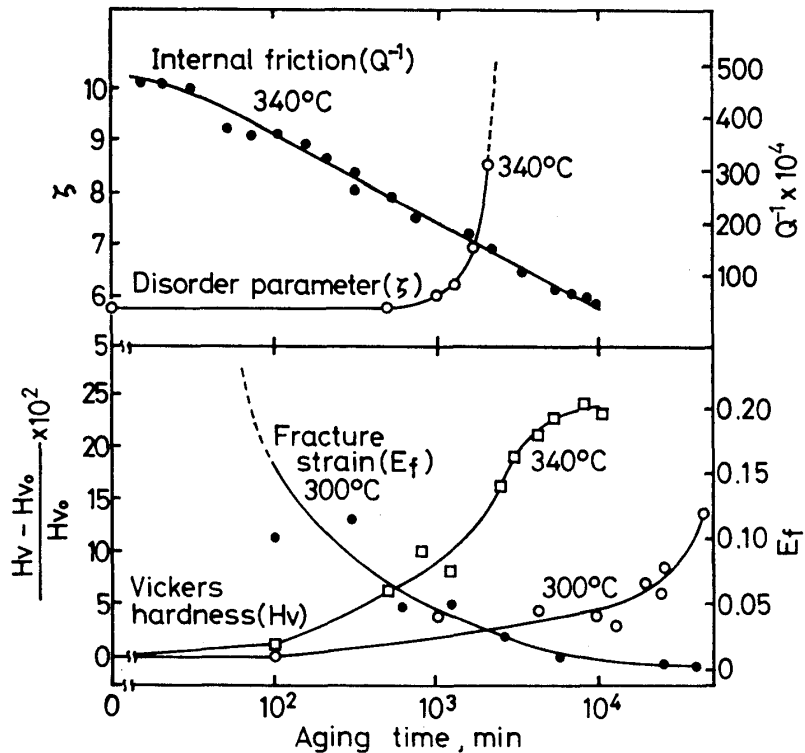


Fig. 9. Changes in various properties of $\text{Fe}_{80}\text{-P}_{13}\text{-C}_7$ alloy during aging at 300° and 340°C.

in the bonding nature between constituent atoms. The embrittlement after aging treatments at lower temperatures is not of a general character of all amorphous alloys but perhaps characteristic to amorphous ferroalloys. This problem will be discussed in near future.

Finally it must be pointed out that the structure relaxation^{(7),(16),(17)} just above room temperature has not been clear within the testing conditions in the present work.

Summary

The thermal instability of amorphous phase and transformation characteristics from amorphous to crystalline phase of several metal-metalloid alloys were investigated by various examinations concerning the structural, physical and mechanical properties. The disorder parameter was introduced in order to estimate the region of short range order.

In temperature-time-transformation diagrams, distinct differences in transformation sequence were obtained above and below the critical temperature. Above this temperature, crystallization proceeds through two metastable phases and finally to the stable phase by nucleation and growth mechanisms. Below the temperature, however, progressive aging gradually changes the structure through

(16) H.S. Chen, J.T. Krause and E. Sigety, *J. Non-Cryst. Solids*, **13** (1973/74), 321.

(17) H.S. Chen, H.J. Leamy and M. Barmatz, *J. Non-Cryst. Solids*, **5** (1971), 444.

two stages. The initial stage corresponds to the incipient stage of crystallization, during which some degree of ordering in atomic arrangements occurs in the amorphous phase. At the subsequent stage the amorphous structure transforms to the single phase, which has the same structure as the constituent metal, in a manner of continuous growth.

Some ordering of atoms in the short range at the incipient stage are reflected in changes of the structure-sensitive properties such as electrical resistivity and internal friction. On the other hand, a remarkable decrease in fracture strain of Fe-P-C alloys occurs after aging treatments at the incipient stage. This phenomenon is not of a general character of all amorphous alloys.